Accepted Manuscript

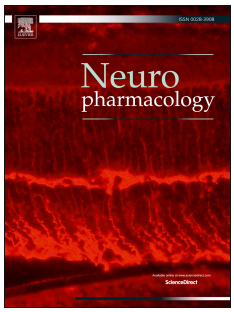

Morphological and functional evidence of increased excitatory signaling in the prelimbic cortex during ethanol withdrawal

Florence P. Varodayan, Harpreet Sidhu, Max Kreifeldt, Marisa Roberto, Candice Contet

PII: S0028-3908(18)30071-6

DOI: 10.1016/j.neuropharm.2018.02.014

Reference: NP 7082

To appear in: *Neuropharmacology*

Received Date: 18 August 2017

Revised Date: 26 January 2018

Accepted Date: 16 February 2018

Please cite this article as: Varodayan, F.P., Sidhu, H., Kreifeldt, M., Roberto, M., Contet, C., Morphological and functional evidence of increased excitatory signaling in the prelimbic cortex during ethanol withdrawal, *Neuropharmacology* (2018), doi: 10.1016/j.neuropharm.2018.02.014.

Morphological and functional evidence of increased excitatory signaling in the prelimbic cortex during ethanol withdrawal

Florence P. Varodayan*, Harpreet Sidhu*, Max Kreifeldt, Marisa Roberto, Candice Contet

*: these authors contributed equally to the work

The Scripps Research Institute, Department of Neuroscience, La Jolla, CA, USA

Corresponding author

Candice Contet

Address: 10550 North Torrey Pines Road, SP40-273, La Jolla, CA 92037, USA

Phone: +1 858 784 7209

Email: contet@scripps.edu

Abstract (222 words)

Excessive alcohol consumption in humans induces deficits in decision making and emotional processing, which indicates a dysfunction of the prefrontal cortex (PFC). The present study aimed to determine the impact of chronic intermittent ethanol (CIE) inhalation on mouse medial PFC pyramidal neurons. Data were collected 6-8 days into withdrawal from 7 weeks of CIE exposure, a time point when mice exhibit behavioral symptoms of withdrawal. We found that spine maturity in prelimbic (PL) layer 2/3 neurons was increased, while dendritic spines in PL layer 5 neurons or infralimbic (IL) neurons were not affected. Corroborating these morphological observations, CIE enhanced glutamatergic transmission in PL layer 2/3 pyramidal neurons, but not IL layer 2/3 neurons. Contrary to our predictions, these cellular alterations were associated with improved, rather than impaired, performance in reversal learning and strategy switching tasks in the Barnes maze at an earlier stage of chronic ethanol exposure (5-7 days withdrawal from 3-4 weeks of CIE), which could result from the anxiety-like behavior associated with ethanol withdrawal. Altogether, this study adds to a growing body of literature indicating that glutamatergic activity in the PFC is upregulated following chronic ethanol exposure, and identifies PL layer 2/3 pyramidal neurons as a sensitive target of synaptic remodeling. It also indicates that the Barnes maze is not suitable to detect deficits in cognitive flexibility in CIE-withdrawn mice.

Key words

medial prefrontal cortex; glutamate; dendritic spines; synaptic transmission; chronic alcohol; abstinence

Introduction

Alcohol use disorders (AUDs) represent a spectrum of pathological patterns of alcoholic beverage consumption, which are notably characterized by loss of control over drinking and the emergence of negative affect during abstinence (American Psychiatric Association, 2013). The transition from moderate alcohol consumption to AUD is characterized by a gradual switch from positive to negative reinforcement, whereby the motivation to drink alcohol is no longer driven by the rewarding effects of intoxication, but by relief from the aversive effects of withdrawal (Cooney et al., 1997; de Castro et al., 2007; Johnson and Fromme, 1994; Lee et al., 2013; Pombo et al., 2016; Sinha, 2013). During abstinence, the heightened incentive salience of alcohol-associated cues combined with deficits in inhibitory control contribute to the reinstatement of drinking (Koob and Volkow, 2016).

Abstinence and cue-induced craving in human alcoholics are associated with abnormal activity in a number of prefrontal cortex (PFC) subregions implicated in reward anticipation, decision making and impulse control, including the dorsolateral PFC, ventromedial PFC, orbitofrontal cortex (OFC) and anterior cingulate cortex (Cyders et al., 2014; Jasinska et al., 2014; Seo et al., 2016). AUDs also cause volume loss and impaired functional connectivity of prefrontal regions (see Dupuy and Chanraud, 2016; Oscar-Berman and Marinkovic, 2007 for reviews). In accordance with these imaging data, AUD subjects exhibit deficits in a number of cognitive processes relevant to decision making and emotional processing (see Le Berre et al., 2017 for review).

Rodents exposed to chronic intermittent ethanol (CIE) also exhibit impaired performance in various cognitive tasks when tested during withdrawal. For instance,

they show deficits in behavioral flexibility (attentional set-shifting and reversal learning in discrimination tasks), excessive impulsivity (premature responding in the 5-choice serial reaction time task), and impaired fear extinction retrieval (Badanich et al., 2011; Holmes et al., 2012; Hu et al., 2015; Irimia et al., 2014; Irimia et al., 2015; Kroener et al., 2012; Trantham-Davidson et al., 2014). Some of these cognitive abilities are known to depend upon medial PFC (mPFC) functional integrity (Chudasama and Robbins, 2006; Dalley et al., 2004; Myers-Schulz and Koenigs, 2012; Seamans et al., 2008; Uylings et al., 2003). Accordingly, studies investigating the molecular basis of the behavioral phenotypes induced by chronic ethanol exposure have identified local changes in excitatory and inhibitory neurotransmission, as well as monoaminergic modulation, within the mPFC (Holmes et al., 2012; Irimia et al., 2017; Kroener et al., 2012; Pleil et al., 2015; Trantham-Davidson et al., 2014). These functional changes are paralleled by structural alterations in dendritic arborization and spines of mPFC pyramidal neurons (Holmes et al., 2012; Kim et al., 2015; Kroener et al., 2012; Navarro and Mandyam, 2015).

The rodent mPFC is subdivided into prelimbic (PL, dorsally located) and infralimbic (IL, ventrally located) areas that exhibit differential connectivity, neurochemistry and behavioral functionality (Dolan and Dayan, 2013; George and Koob, 2010; Gourley and Taylor, 2016; Heidbreder and Groenewegen, 2003; Moorman et al., 2015; Vertes, 2004). In instrumental learning the PL and IL cortices promote mutually exclusive behaviors such that goal-directed actions require the PL area, while habitual responding requires the IL area (Balleine and Dickinson, 1998; Coutureau and Killcross, 2003; Killcross and Coutureau, 2003). The antagonistic functions of the PL and IL cortices are best illustrated by fear conditioning experiments, whereby the expression of learned fear

is reduced both by PL inactivation or IL stimulation, while the extinction of conditioned freezing response is prevented both by IL inactivation or PL stimulation (Milad and Quirk, 2002; Morgan and LeDoux, 1995; Quirk et al., 2000; Vidal-Gonzalez et al., 2006). A similar distinction between behavioral execution and inhibition being driven by the PL and IL cortices, respectively, has also been proposed for reward/drug seeking, although the dichotomy appears less rigid than for aversive conditioning (Moorman et al., 2015; Peters et al., 2009; Pfarr et al., 2015). Finally, the PL and IL cortices play complementary roles in behavioral flexibility and conflict resolution; the IL facilitates the testing of a previously irrelevant strategy upon rule-shifting and reversal learning, while the PL enables the selection and maintenance of the new strategy (Oualian and Gisquet-Verrier, 2010). In accordance with this functional dichotomy, the few studies that have examined ethanol-induced neuroadaptations in both the PL and IL cortices have observed differential alterations of dendritic spines and synaptic transmission in the two subregions (Gass et al., 2014; Jury et al., 2017b; Pleil et al., 2015).

The mPFC is also laminar, with superficial (2/3) and deeper (5) layers exhibiting differential connectivity (Bitzenhofer et al., 2017; DeNardo et al., 2015; Gabbott et al., 2005). While there is *in vitro* evidence of layer specificity in the effects of chronic ethanol on mPFC pyramidal neurons (Pava and Woodward, 2014), there is no study to date that has directly compared neuroadaptations occurring in layer 2/3 vs layer 5 neurons *in vivo*.

Therefore, the present study aimed to: 1) investigate spine alterations in layer 2/3 and layer 5 pyramidal neurons of the PL and IL cortices of CIE-exposed mice, 2) determine whether morphological changes were associated with alterations in intrinsic excitability

or excitatory synaptic transmission, and 3) assess whether cellular changes were associated with deficits in cognitive flexibility as measured by reversal learning and strategy switching in the Barnes maze. Data were collected 3-8 days into withdrawal from vapor, a time frame when CIE-exposed mice display escalated ethanol drinking and other behavioral alterations (Becker and Lopez, 2004; Jury et al., 2017a; Kroener et al., 2012).

Materials and Methods

Animals. Male C57BL/6J mice were obtained from The Scripps Research Institute Rodent Breeding Colony at 8 weeks of age and were acclimated to reverse light cycle (12 h light/dark cycle, lights on at 10:15 PM) for at least 10 days before any testing or treatment was performed. Mice were housed in a temperature-controlled vivarium (22°C). Water (acidified) and food (autoclaved Teklad LM-485/ Envigo 7012 diet) were available *ad libitum*. All procedures were carried out in accordance with the National Institutes of Health *Guide for the Care and Use of Laboratory Animals* and were approved by The Scripps Research Institute Institutional Animal Care and Use Committee.

Chronic intermittent exposure to ethanol vapor (CIE). Inhalation chambers (La Jolla Alcohol Research Inc., La Jolla, CA) consisted of standard plastic mouse cages closed with airtight lids and fitted with two inlets for ethanol vapor inflow in the front and passive exhaust in the back. Ethanol vapor was created by dripping 95% ethanol into a 2-L Erlenmeyer vacuum flask kept at 50°C on a warming tray. Air was pumped into the flask (HK40L, Hakko, Laguna Hills, CA) and ethanol vapor flowed into each sealed chamber at a rate of 6 L/min. During each CIE week, mice were placed in inhalation chambers and subjected to four cycles of intoxication (ethanol vapor inhalation for 16 h, from 5:00 PM to 9:00 AM, starting Monday afternoon and ending Friday morning) separated by 8 h periods of withdrawal (air inhalation), and then returned to their home cage. Before each onset of ethanol vapor exposure, mice were injected intraperitoneally with a solution of ethanol (1.5 g/kg) and pyrazole (1 mmol/kg, Sigma, St Louis, MO), with control mice receiving injections of pyrazole alone. Ethanol vapor concentration was

adjusted by varying the ethanol dripping rate, so as to yield serum ethanol concentrations approximating 200 mg/dL. Blood samples were obtained once per week at the end of a 16 h intoxication period. Blood was collected from the tail vein with heparinized capillary tubes and centrifuged for 5 min at 13000 rpm. The supernatant was processed in a GM7 analyser (Analox Instruments, London, UK). Average serum ethanol concentration was 217.5 ± 22.6 mg/dL in the cohort used for dendritic spine analysis, 211.8 ± 19.0 mg/dL in the cohort used for electrophysiological recordings, and 208.8 ± 14.3 mg/dL in the cohorts used for Barnes maze testing.

Dendritic spine analysis. Mice (Air, n=4; CIE, n=5) were exposed to a total of 7 weeks of air/CIE and euthanized 7 days into withdrawal. Mice were anesthetized with isoflurane and perfused with cold PBS followed by 4% paraformaldehyde (PFA). Brains were extracted and postfixed in 4% PFA at 4^{o}C for 2 hours before being sectioned coronally into 100 µm slices on a vibratome (Leica VT1000S; Leica Biosystems). Sections were then labeled with 1,1′-dioctadecyl-3,3,3′,3′-tetramethylindocarbocyanine perchlorate (DiI) using a biolistic delivery system (Helios Gene Gun, Biorad) and incubated in PBS for 3 days at 4^{o}C before being mounted onto slides in PBS. Neurons in layers 2/3 and 5 of the prelimbic (PL) and infralimbic (IL) divisions of the mPFC were imaged by confocal microscopy (model LSM 710; Carl Zeiss MicroImaging) using a series of high-resolution optical sections (1,024 × 1,024-pixel format) that were captured for each neuron with a 63× water-immersion objective (1.2 numerical aperture), with 1x zoom at 1-µm step intervals (z-stack). All images were acquired under identical conditions. Each z-stack was collapsed into a single image by projection in Zeiss ZEN software, converted to a tiff file, encoded for blind analysis and spine counting was

performed in Image J (NIH). Sections from at least 20 cells and between 40-58 dendritic segments were imaged per treatment condition.

Electrophysiological recordings. Mice (Air, n=5; CIE, n=5) were exposed to a total of 7 weeks of air/CIE and euthanized 6-8 days into withdrawal. After euthanasia with 3-5% isoflurane, the brains were placed in cold, oxygenated (95% O_2/5% CO_2) high sucrose solution (pH 7.3-7.4): 206.0 mM sucrose; 2.5 mM KCl; 0.5 mM $CaCl_2$; 7.0 mM $MgCl_2$; 1.2 mM NaH_2PO_4; 26.0 mM $NaHCO_3$; 5.0 glucose; 5.0 HEPES, as previously described (Bajo et al., 2015; Salling and Harrison, 2014; Schweitzer et al., 2016). Coronal slices (300 µm) containing the PL and IL cortices were sectioned (Leica VT1000S) and incubated in oxygenated artificial cerebrospinal fluid: 130 mM NaCl, 3.5 mM KCl, 2 mM $CaCl_2$, 1.25 mM NaH_2PO_4, 1.5 mM $MgSO_4$, 24 mM $NaHCO_3$, and 10 mM glucose for 30 min at 32 °C and then for 30 min at room temperature. PL and IL neurons were visualized with infrared-differential interference contrast (IR-DIC) optics, a w60 water immersion objective (Olympus BX51WI) and a CCD camera (EXi Aqua, QImaging), and layer 2/3 pyramidal neurons located 100-300 µm from the pial surface were identified by their characteristic size and shape (Salling and Harrison, 2014). Whole-cell recordings from a total of 175 neurons were performed in gap-free acquisition mode with a sampling rate per signal of 20 kHz and low-pass filtered at 10 kHz, using a Multiclamp 700B amplifier, Digidata 1440A and pClamp 10.2 software (all Molecular Devices). Recording pipettes (4-6 MΩ resistance) were filled with internal solution: 145 mM K-gluconate, 0.5 mM EGTA, 2 mM $MgCl_2$, 10 mM HEPES, 2 mM Na-ATP, and 0.2 mM Na-GTP. Neuronal membrane properties (resting membrane potential and input resistance) and excitability (action potential threshold and rheobase, recorded in

current-clamp mode using a series of current injections of 5 pA/600 ms in cells held at -70 mV) were assessed, and the recordings analyzed using NeuroExpress software developed by Dr. A. Szucs. For the voltage-clamp experiments, cells held at -70 mV were bathed in GABA receptor antagonists (1 µM CGP 55845A and 30 µM bicuculline) to isolate spontaneous glutamatergic excitatory postsynaptic currents (sEPSCs). Due to the magnesium concentration in the ACSF and our cell holding potential, we expect these sEPSCs to be primarily AMPA receptor-mediated currents. To confirm this, the NMDA receptor antagonist DL-2-Amino-5-phosphonopentanoic acid (30 µM DL-AP5) was subsequently applied to the bath in a subset of recordings from PL and IL neurons of Air and CIE mice. sEPSC recordings with a series resistance >15 MΩ or a >20% change in series resistance, as monitored with a 10 mV pulse, were excluded. sEPSC frequencies, amplitudes and kinetics were analyzed over a 3 min period using Mini Analysis software (Synaptosoft Inc.) and visually confirmed, with events <5 pA excluded and cells with less than 60 events/3 min interval excluded.

Barnes maze. Two independent cohorts of mice were tested in the Barnes maze to examine cognitive flexibility 5-7 days into withdrawal from 3-4 weeks of CIE exposure (first cohort, n=24 mice; second cohort, n=12 mice). The Barnes maze test was performed as described previously (Bach et al., 1995; Barnes, 1979; Holmes et al., 2002; Sunyer et al., 2007). Mice were given 5 min to escape into a small dark recessed chamber placed under 1 of 20 small holes (2” diameter) evenly distributed along the perimeter of an elevated (36” high), brightly lit (400 lux), circular open platform (36” diameter). At the beginning of each trial, the mouse was placed in the center of the maze under an opaque cylinder (4” high). After 10 s, the cylinder was lifted and the trial

began. Once the mouse entered the escape box, the hole was covered to prevent the mouse from resurfacing onto the maze and the mouse was returned to its home cage 1 min later. If the mouse failed to enter the escape box within 5 min, it was gently guided toward the target hole and allowed to enter the escape box. Mice were given two trials per day, the first at the beginning of the dark phase and the second approximately 3 h later. A habituation session was first performed, which entailed placing the mouse in the escape box for 1 min. The mice then underwent four testing phases: spatial learning, memory retention/re-acquisition, reversal learning and strategy switching (**Fig. 5A**). During the acquisition phase, the location of the escape box was constant for a given mouse (but randomized across mice), and distal visual cues were available for the mouse to navigate. The path of the mouse was recorded by a ceiling-mounted video camera linked to Any-maze video tracking software (Stoelting). The time elapsed, distance traveled, and number of holes visited prior to entering the escape box were used as performance indexes. Path length was the primary endpoint as this measure is not confounded by velocity (Contet et al., 2001). Mice were tested as many times as needed for their performance to stabilize and for their search strategy to be serial or direct rather than random (20 trials in first cohort, 24 trials in second cohort). One mouse was excluded because it systematically jumped from the platform and five other mice were excluded because they were still using a random strategy by the end of the acquisition phase. Mice were then exposed to three weeks of air (n=14) or CIE (n=16) inhalation. Five mice died 24-72 h into withdrawal after their first week of CIE exposure. After three air/CIE weeks, a Barnes maze trial was conducted 3 days into withdrawal from vapor to assess spatial memory retention. Mice were then retrained under the

same conditions until their performance stabilized (5 trials, withdrawal days 3-5). The reversal learning phase was then started, whereby the location of the escape box was moved to the hole diametrically opposed to the hole used during the acquisition phase. Mice were then tested until their performance stabilized (5 trials, withdrawal days 5-7). The mice were then exposed to one more week of air or CIE inhalation, and a Barnes maze trial was conducted 3 days into withdrawal from vapor using the same conditions as during the reversal learning phase. Mice were then retrained under the same conditions until their performance stabilized (6 trials, withdrawal days 3-5). The strategy switching phase was then started, whereby a beacon (orange plastic racket-shaped toy, 3.5" high, 2" wide) was affixed on the rim of the platform, next to the escape hole, and the location of the escape hole changed at every trial (i.e., mice now had to rely on a proximal cue rather than distal cues for navigation). Mice were then tested until their performance stabilized (5 trials, withdrawal days 5-7). Mice from the second cohort were then exposed to an additional 3 weeks of CIE following completion of the Barnes maze experiment and were used for dendritic spine analysis.

Data analysis

Spine densities and electrophysiological measures were analyzed by unpaired two-tailed t-tests. Spine proportions were analyzed using two-way repeated-measures analysis of variance (ANOVA), with spine shape as the within-subject variable and treatment as the between-subject variable. Barnes maze data were analyzed by two-way repeated-measure ANOVA, with trial as the within-subject variable and treatment as the between-subject variable. Simple linear regression was performed to correlate dendritic spine parameters with cognitive flexibility performance in the Barnes maze,

using the average distance traveled during all reversal learning and strategy switching trials as the independent variable. Data are presented as mean ± standard error of the mean (SEM), with the number of cells and mice used for each experiment reported in the figure legend.

Results

CIE increases the maturity of dendritic spines in PL layer 2/3 pyramidal neurons. We examined whether CIE exposure followed by 7 days of withdrawal produced dendritic spine remodeling in layer 2/3 and layer 5 pyramidal neurons of the PL and IL cortices. CIE did not alter spine density in either layer of both subregions (**Fig. 1**). We further analyzed the morphology of dendritic protrusions, which were classified as mushroom (most mature), stubby, thin and filopodia (least mature) (**Fig. 2A**). There was a significant interaction between spine type and treatment in PL layer 2/3 neurons ($F_{3,21}$ = 8.0, $p<0.001$), whereby CIE increased the proportion of mushroom spines ($p<0.01$) and decreased the proportion of thin spines ($p<0.01$) (**Fig. 2B**). A similar interaction was observed in IL layer 2/3 neurons ($F_{3,21}$ = 3.2, $p<0.05$), but *post hoc* analysis did not detect a significant change in the proportion of any spine type (**Fig. 2D**). There were no significant changes in the proportions of spine types in PL and IL layer 5 neurons (**Fig. 2C** and **2E**).

CIE does not affect the basal membrane properties or excitability of PL layer 2/3 pyramidal neurons. To determine whether the region- and layer-specific effect of CIE on spine maturity was associated with altered neuronal function, we performed *in vitro* whole-cell electrophysiology in PL and IL layer 2/3 pyramidal neurons 6-8 days into withdrawal from CIE (**Fig. 3A**). In both mPFC subregions, there were no differences in resting membrane potential, input resistance, action potential threshold and rheobase between control and CIE-exposed mice (**Fig. 3B-J**), indicating that CIE did not affect neuronal membrane properties or excitability.

CIE increases postsynaptic glutamate receptor function at PL layer 2/3 synapses. We then investigated whether CIE altered glutamatergic signaling at PL and IL layer 2/3 synapses by recording pharmacologically-isolated spontaneous excitatory postsynaptic currents (sEPSCs). In PL layer 2/3 pyramidal neurons, CIE-exposed mice displayed a similar sEPSC frequency to that of control mice, but had a significantly higher sEPSC amplitude (t_{45}=3.31, p<0.01; **Fig. 4A-C**). There was also a significant increase in the sEPSC decay time of PL layer 2/3 pyramidal neurons after exposure to CIE (t_{45}=3.10, p<0.01; **Fig. 4A** and **4D**). In contrast, CIE had no effect on the sEPSC frequency, amplitude or kinetics of IL layer 2/3 pyramidal neurons (**Fig. 4E-H**). Generally, increased sEPSC frequencies reflect higher glutamate release probabilities, whereas increased amplitudes and kinetics indicate enhanced glutamate receptor sensitivity (via changed receptor number and/or subunit composition) (De Koninck and Mody, 1994; Otis et al., 1994). Therefore, CIE increased postsynaptic glutamate receptor function at PL layer 2/3 synapses, but not IL layer 2/3 synapses, without affecting glutamate release in either subregion. These postsynaptic effects were primarily mediated by AMPA receptors, as the NMDA receptor antagonist DL-AP5 (30 μM) was applied to a subset of recorded cells (n=16 cells from both subregions of Air and CIE mice) and no differences in sEPSC characteristics were observed (**Supplementary Figure S1**).

CIE does not impair memory retention, reversal learning or strategy switching in the Barnes maze. We sought to identify a behavioral correlate of the morphological and functional changes identified in PL layer 2/3 pyramidal neurons. To do so, we evaluated the effect of CIE on cognitive flexibility in the Barnes maze spatial reference memory assay (**Fig. 5A-B**). We first trained the mice to learn the location of the escape hole

using distal cues. We then exposed the mice to 3 consecutive weeks of air or CIE inhalation. Both groups showed an equivalent reduction in performance (as measured by path length) at the first post-CIE trial (effect of trial, $F_{1,23}$=5.6, $p<0.05$; effect of treatment, $F_{1,23}$=0.2, n.s.; trial x treatment, $F_{1,23}$=0.004, n.s.) and re-acquired the task at the same rate (effect of trial, $F_{4,92}$=6.8, $p<0.001$; effect of treatment, $F_{1,23}$=1.6, n.s.; treatment x trial interaction, $F_{4,92}$=2.2, n.s.). We then assigned the target hole to the diametrically opposite location for each mouse (reversal learning phase, withdrawal days 5-7). Both groups showed an equivalent reduction in performance at the first reversal learning trial (effect of trial, $F_{1,23}$=23.4, $p<0.001$; effect of treatment, $F_{1,23}$=0.3, n.s.; treatment x trial interaction, $F_{1,23}$=1.9, n.s.). Both groups learned the new location at the same rate but CIE-exposed mice performed better throughout the reversal learning phase (effect of trial, $F_{4,92}$=5.9, $p<0.001$; effect of treatment, $F_{1,23}$=5.1, $p<0.05$; treatment x trial interaction, $F_{4,92}$=0.4, n.s.). The mice were then exposed to an additional week of air or CIE inhalation. There was no significant effect of the 10-day testing pause on performance (effect of trial, $F_{1,23}$=2.2, n.s.; effect of treatment, $F_{1,23}$=0.3, n.s.; treatment x trial interaction, $F_{1,23}$=0.01, n.s.). Both groups improved their performance at the same rate during re-acquisition trials, but the CIE-exposed mice again performed better than their air-exposed counterparts throughout re-acquisition (effect of trial, $F_{5,115}$=2.4, $p<0.05$; effect of treatment, $F_{1,23}$=4.2, $p=0.05$; treatment x trial interaction, $F_{5,115}$=0.1, n.s.). We then randomly changed the location of the target hole at each trial and signaled the target hole with a proximal cue (strategy switching phase, withdrawal days 5-7). Both groups showed a major reduction in performance at the first strategy-switching trial, but CIE-exposed mice again performed better (effect of trial,

$F_{1,23}$=26.3, p<0.001; effect of treatment, $F_{1,23}$=6.6, p<0.05; treatment x trial interaction, $F_{1,23}$=2.5, n.s.). Both groups learned the new strategy at the same rate (effect of trial, $F_{4,92}$=2.9, p<0.05; effect of treatment, $F_{1,23}$=4.1, p=0.056; treatment x trial interaction, $F_{4,92}$=0.5, n.s.). Similar data were obtained using latency to escape or number of holes visited as a measure of performance (**Supplementary Figure S2A-B** and **Tables S1-S2**).

Dendritic spine morphology in PL layer 2/3 pyramidal neurons correlates with Barnes maze performance. Finally, we examined whether the performance of mice during cognitive flexibility testing predicted dendritic spine morphology after exposure to an additional 3 weeks of CIE and 7 days of withdrawal. For PL layer 2/3 neurons, the average distance traveled during reversal learning and strategy switching trials was negatively correlated with the percentage of mushroom spines (R^2=0.594, p<0.05) and positively correlated with the percentage of thin spines (R^2=0.587, p<0.05). There was also a trend for a negative correlation with spine density (R^2=0.551, p=0.056). There was no significant correlation with any of the spine parameters measured in the other populations of mPFC pyramidal neurons.

Discussion

Our study shows that chronic exposure to ethanol followed by one week of withdrawal elicits morphological and functional changes indicative of enhanced AMPA receptor-mediated excitatory transmission in layer 2/3 pyramidal neurons of the PL subregion of the mouse mPFC. Specifically, we found that subjecting mice to 7 weeks of CIE followed by 6-8 days of withdrawal did not affect dendritic spines in PL layer 5 neurons or IL neurons, but selectively increased spine maturity in PL layer 2/3 neurons. While there was no effect of CIE on basal membrane properties or excitability of layer 2/3 pyramidal neurons in either mPFC subregion, CIE increased the postsynaptic glutamate receptor function of PL layer 2/3 neurons, but not IL layer 2/3 neurons, and this effect was primarily mediated by AMPA receptors. Contrary to our predictions, these cellular alterations were associated with improved, rather than impaired, performance in reversal learning and strategy switching tasks in the Barnes maze, and there was a positive correlation between PL layer 2/3 spine maturity and cognitive flexibility.

Spine morphology plays a critical role in regulating excitatory synaptic function, as the maturation of dendritic spines and enlargement of spine heads is associated with increased spine stability and increased synaptic strength (De Roo et al., 2008; Sala and Segal, 2014). Mushrooms spines have larger postsynaptic densities, which anchor more AMPA receptors and make these synapses functionally stronger (Bourne and Harris, 2007). Accordingly, chronic ethanol binge drinking increased the average spine area and the proportion of mushroom spines in medium spiny neurons of the nucleus accumbens shell, and these changes were associated with the insertion of GluA2-lacking AMPA receptors (Laguesse et al., 2017). Another critical component of ethanol-

induced plasticity at glutamatergic synapses involves the upregulation of synaptic NR2B-containing NMDA receptors and subsequent expansion of the postsynaptic density via PSD-95 scaffolding capacity (Kroener et al., 2012; Mulholland and Chandler, 2007). In our study, withdrawal from CIE increased the proportion of mushroom spines at the expense of thin spines selectively in PL layer 2/3 neurons. In agreement with the known relationship between spine shape and function, these structural changes were accompanied by an increase in sEPSC amplitude and decay time, which reflects enhanced postsynaptic glutamate receptor function and was primarily mediated by AMPA receptors as our recording conditions did not allow for the measure of NMDA receptor-mediated currents. Importantly, CIE did not affect spine maturity nor excitatory transmission in IL layer 2/3 pyramidal neurons, which further supports the correlation between spine morphology and synaptic function.

Our morphological and functional results therefore add to a growing body of literature indicating that glutamatergic activity in the PFC is upregulated following chronic ethanol exposure (see Burnett et al., 2016 for review). Importantly, we observed a higher sensitivity of PL layer 2/3 neurons compared to layer 5 or IL neurons. This finding corroborates a recent study by Jury et al. that reported no changes in total spine density in mouse PL and IL layer 2/3 neurons, but a selective increase in the head width of wide spines on PL layer 2/3 neurons (i.e., mushroom spines, based on the classification we used in the present study) after 3 days of withdrawal from CIE (Jury et al., 2017b). In contrast to these and our data, CIE-exposed rats exhibited a higher overall spine density, but no change in mushroom spine density, in mPFC layer 2/3 neurons (PL and IL neurons were not distinguished) 3 h after the last vapor exposure (Kim et al., 2015).

Possible explanations for this divergent finding include the different species and different withdrawal time-point used in that study. Likewise, Pleil and colleagues reported a trend for increased sEPSC amplitude in mouse PL layer 2/3 neurons recorded 48 h into withdrawal from three weeks of CIE (Pleil et al., 2015), and it is possible that this trend would have reached significance had the mice experienced longer CIE exposure and/or withdrawal as in the present study. Finally, in an earlier report, CIE increased spine maturity in mouse mPFC layer 5 neurons and this increase persisted after one week of withdrawal, which we did not replicate in our study (Kroener et al., 2012). Although the experimental conditions were for the most part identical to those used here, we speculate that the discrepancy arises from a differential extent of CIE exposure (three weeks in Kroener et al., 2012 vs seven weeks in the present study), which may correspond to different stages of ethanol dependence. Further studies will be needed to address the molecular mechanisms underlying increased spine maturity and glutamatergic transmission in PL layer 2/3 neurons following CIE exposure. A promising approach would entail the proteomic analysis of synaptic fractions, as was recently done in the nucleus accumbens and hippocampus (Uys et al., 2016; Wills et al., 2017). These pioneering studies identified a number of scaffolding proteins, cytoskeletal proteins, and other proteins known to regulate cellular morphology, which may contribute to dendritic spine plasticity during ethanol intoxication and withdrawal.

Based on the morphological and functional alterations we detected in PL layer 2/3 pyramidal neurons, we predicted that CIE-exposed mice would show impaired cognitive flexibility in the Barnes maze. Although spatial reference learning and memory is

primarily dependent on the hippocampus, behavioral flexibility in spatial navigation tasks requires the mPFC (de Bruin et al., 1994; Deacon et al., 2002; Deacon and Rawlins, 2002; Delatour and Gisquet-Verrier, 2000; Lacroix et al., 2002; Latif-Hernandez et al., 2016; Livingston-Thomas et al., 2015; McDonald et al., 2008; Morris et al., 1982; Ragozzino et al., 1999). In particular, mPFC lesions in the rat impair reversal spatial learning and shifting from a spatial to a visual strategy in the Morris water maze (de Bruin et al., 1994; Ragozzino et al., 1999). Our experimental design aimed to detect CIE-induced mPFC deficits by testing these two aspects of cognitive flexibility in a spatial navigation task. We selected the Barnes maze because it is less stressful for mice than the Morris water maze (as measured by plasma corticosterone levels) and the spatial learning ability of mice is higher in dry-land tasks than in swimming-pool tasks (Harrison et al., 2009; Whishaw and Tomie, 1996). A limitation of our study is that cognitive flexibility was examined after 3-4 weeks of CIE, while cellular analyses were conducted after 7 weeks of CIE. Despite this discrepancy, Barnes maze performance during reversal learning and strategy switching predicted dendritic spine maturity in PL layer 2/3 neurons, but not other populations of mPFC pyramidal neurons.

Overall, we found that CIE exposure reduced Barnes maze performance to the same extent as an equivalent break in training in air-exposed mice, indicating that CIE does not affect the retention of spatial reference memory. This result is consistent with the lack of effect of CIE on the retention of previously learned discrimination tasks (Badanich et al., 2011; Kroener et al., 2012). In contrast, our observation that CIE-exposed mice performed as well, or even better, than their air-exposed counterparts in the reversal learning and strategy switching phases of the Barnes maze experiment is

at odds with studies that detected impaired cognitive flexibility in discrimination tasks 3-7 days into withdrawal from 3 weeks of CIE (Badanich et al., 2011; Kroener et al., 2012). Several possibilities can be considered to explain the incongruity between our results and those previous reports.

First, distinct experimental procedures of cognitive flexibility assessment are known to engage different prefrontal subregions, which may be differentially impacted by CIE (Dalley et al., 2004). For instance, in tasks using distinct sensory modalities, the PL is critical for attentional processes related to visual inputs, while the OFC processes olfactory and gustatory information (see Uylings et al., 2003 for review). Furthermore, reversal learning in simple discrimination tasks recruits the OFC, while the mPFC is necessary for reversal learning in spatial navigation tasks, as well as for task shifts that involve more effortful processing ("higher order rules") (Brown and Bowman, 2002; Chudasama and Robbins, 2006; de Bruin et al., 1994; Floresco et al., 2008). In support of this view, reversal learning and attentional set-shifting deficits previously reported in CIE-exposed mice were identified using distinct procedures. Badanich et al. used an odor + digging medium discrimination task and detected deficits in reversal learning, but not set-shifting, 3 days into withdrawal from CIE (Badanich et al., 2011). In contrast, Kroener and colleagues used a T-maze discrimination task based on either egocentric response or visual cue and detected deficits in set-shifting, but not reversal learning, 3-7 days into withdrawal (Hu et al., 2015; Kroener et al., 2012). Deficits in attentional set-shifting were also observed in CIE-exposed rats tested in an operant discrimination task (Trantham-Davidson et al., 2014). Our data indicate that the Barnes maze is not suitable to detect either type of CIE-induced deficit in cognitive flexibility, even though it

revealed reversal learning deficits in adult mice exposed to ethanol binges during adolescence (Coleman et al., 2014). Although the mPFC is critical to cognitive flexibility in spatial navigation tasks, it is possible that the particular mPFC neurons recruited during task shifts are not those affected by CIE, namely PL layer 2/3 pyramidal neurons.

Our data may also result from counterintuitive consequences of mPFC dysfunction. In contrast to the effect of larger thermal lesions of the mPFC, electrolytic lesions confined to the PL cortex paradoxically improved reversal learning in the Morris water maze (de Bruin et al., 1994; Maaswinkel et al., 1996). This observation is particularly relevant to our observation of the selective impact of CIE on PL pyramidal neurons, rather than IL pyramidal neurons. The improved performance of CIE-exposed mice during the reversal learning and strategy switching phases may therefore be compatible with PL cortex dysfunction. Interestingly, CIE-exposed mice also performed slightly better in the intra-dimensional shift test conducted after reversal learning by Badanich et al., indicating a modest facilitation of cognitive flexibility in that particular task switch (Badanich et al., 2011). Further studies will be needed to elucidate how increased excitatory transmission in PL pyramidal neurons may produce behavioral phenotypes similar to those elicited by mPFC inactivation. A similar situation was previously observed in a mouse model of traumatic brain injury, whereby increased glutamatergic input onto PL layer 2/3 (but not layer 5) pyramidal neurons was associated with working memory deficits (Smith et al., 2015). Moreover, increased excitatory transmission may not necessarily increase neuronal activity *in vivo* and may instead be associated with hypoactivity, i.e., comparable to the effects of experimental inactivation. An example of such dissociation was reported in inflammatory and neuropathic pain models, whereby

PL layer 2/3 pyramidal neuron dendritic branching, spine density and glutamatergic synaptic transmission were increased, yet the excitability of these neurons was reduced and the associated behavioral phenotypes were reversed by optogenetic activation of PL excitatory neurons (Metz et al., 2009; Wang et al., 2015).

A third possible explanation for the discrepancy between our data and previous findings relates to the potential interference of other behavioral alterations elicited by CIE withdrawal (e.g., negative emotional state) with Barnes maze performance. Importantly, in the studies by Badanich et al. and Kroener et al. mice were motivated to complete the cognitive task by earning a reward (palatable food), while in our study mice were motivated by escaping an aversive environment (brightly lit, open space). Anxiety-like behavior is therefore more likely to have influenced performance in our study by increasing motivation to locate the escape hole. In accordance with this hypothesis, CIE-exposed male mice exhibit anxiety-like behavior 3-6 days into withdrawal and may therefore be more sensitive to the aversive nature of the Barnes maze (Jury et al., 2017a). Interestingly, mPFC layer 2/3 neurons have been implicated in moderating the impact of stress on emotions (Shrestha et al., 2015). The cellular abnormalities we identified in this neuronal population could therefore promote anxiety in CIE-exposed mice. Layer 2/3 pyramidal neurons of the mouse PL cortex receive inputs from the contralateral mPFC, basolateral amygdala, midline thalamic nucleus and ventral hippocampus, indicating that CIE may increase excitatory drive from these areas to elicit anxiety (Cheriyan et al., 2016; Little and Carter, 2012).

Of note, the phenotype we observed in the Barnes maze may not necessarily generalize to other spatial navigation tasks. Anxiety-like behavior and plasma

corticosterone levels negatively correlate with Morris water maze performance (Darcet et al., 2014; Harrison et al., 2009; Holscher, 1999; Miyakawa et al., 2001), suggesting that the anxiogenic-like effects of CIE withdrawal would likely worsen reversal learning abilities in this task. While this interaction has yet to be studied, the reversal learning deficits induced by adolescent ethanol binge drinking can be detected both in the Barnes and Morris water mazes, despite the presence of an anxious-like phenotype (Coleman et al., 2011; Coleman et al., 2014). Our results, in conjunction with these findings, indicate that adolescent binge drinking and adult CIE elicit distinct cognitive alterations.

Collectively, we have shown that glutamatergic activity in the PFC is upregulated following chronic ethanol exposure, and identified PL layer 2/3 pyramidal neurons as a sensitive target of synaptic remodeling. In the future, it will be interesting to determine whether inhibition (or activation) of PL pyramidal neurons can reverse some of the behavioral consequences of CIE. Further insights into the chain of events linking the PL cortex to cognitive and emotional disruption during ethanol withdrawal may also be provided by studying the impact of CIE on downstream circuitry, i.e., on those neurons whose activity is controlled by PL layer 2/3 pyramidal neurons, such as ventral striatum or basolateral amygdala neurons (Gabbott et al., 2005; Little and Carter, 2013).

Figure legends

Figure 1. Spine density in layer 2/3 and 5 of the prelimbic (PL) and infralimbic (IL) divisions of the medial prefrontal cortex. A: Representative image of the dendrites imaged and analyzed. **B-E:** Spines were analyzed in pyramidal neurons of PL layer 2/3 (B) and layer 5 (C) and IL layer 2/3 (D) and layer 5 (E). Spine densities were analyzed by unpaired t-test and no effect of CIE was detected. Data are presented as mean ± SEM (Air, n=40 dendritic segments from 15 neurons from 4 mice; CIE, n=58 dendritic segments from 16 neurons from 5 mice).

Figure 2. Proportion of spine types in layer 2/3 and 5 of the prelimbic (PL) and infralimbic (IL) divisions of the medial prefrontal cortex. A: Schematic showing the classification of the different spine types. **B-E:** Spine type proportions were analyzed using repeated measures ANOVA and there was a significant interaction between spine type and treatment in PL layer 2/3 ($F_{3,21}$=8.0, $p<0.001$) (B) and IL layer 2/3 neurons ($F_{3,21}$=3.2, $p<0.05$) (D), but not in PL layer 5 (C) or IL layer 5 neurons (E). **, $p<0.05$. Data are presented as mean ± SEM (Air, n=40 dendritic segments from 15 neurons from 4 mice; CIE, n= 58 dendritic segments from 16 neurons from 5 mice).

Figure 3. Membrane properties and excitability measures in layer 2/3 neurons of the prelimbic (PL) and infralimbic (IL) cortices. A: Schematic illustrating the location of PL and IL areas (left panel). Pipettes were directed at layer 2/3 (×4, middle panel), and pyramidal neurons were identified by their triangular shape with IR-DIC optics (×60, right panel). **B-C:** Group comparison by unpaired t-test showed no differences in the resting membrane potential (B) or input resistance (C) of PL layer 2/3 pyramidal neurons between control and CIE mice (Air, n=28 cells from 5 mice; CIE, n=25 cells

from 5 mice). **D:** Representative traces of current-injected firing elicited by a stimulus waveform (5 pA steps, 600 ms duration) from PL layer 2/3 pyramidal neurons in control and CIE mice. The depicted sweeps resulted from injection of 0, 20, 40, 60, 80, 100, 120, 140, 160, 180 and 200 pA into both cells. **E-F:** Group comparison by unpaired t-test showed no differences in the action potential threshold (E) or rheobase (F) of PL layer 2/3 pyramidal neurons in control and CIE mice (Air, n=28 cells from 5 mice; CIE, n=25 cells from 5 mice). **G-J:** Group comparison by unpaired t-test showed no differences in the resting membrane potential (G), input resistance (H), action potential threshold (I) or rheobase (J) of IL layer 2/3 pyramidal neurons between control and CIE mice (Air, n=24 cells from 5 mice; CIE, n=27 cells from 5 mice). Data are presented as mean ± SEM.

Figure 4. Glutamatergic transmission in layer 2/3 neurons of the prelimbic (PL) and infralimbic (IL) cortices. A: Representative sEPSC traces (left panel) and scaled average sEPSCs (right panel) from PL layer 2/3 pyramidal neurons of control and CIE mice. **B-D:** Group comparison by unpaired t-test showed no difference in baseline sEPSC frequency (B), but a significantly higher sEPSC amplitude (C) and decay time (D) in CIE vs. control mice (Air, n=24 cells from 5 mice; CIE, n=23 cells from 5 mice). **E:** Representative sEPSC traces (left panel) and scaled average sEPSCs (right panel) from IL layer 2/3 pyramidal neurons of control and CIE mice. **F-H:** Group comparison by unpaired t-test showed no differences in baseline sEPSC frequency (F), amplitude (G) and kinetics (H) in CIE vs. control mice (Air, n=24 cells from 5 mice; CIE, n=24 cells from 5 mice). Data are presented as mean ± SEM. **, $p<0.01$.

Figure 5. Effect of CIE on spatial reference memory retention and cognitive flexibility in the Barnes maze. A: Experimental design. Mice were first trained to acquire the spatial navigation task, then exposed to three weeks of air or chronic intermittent ethanol (CIE, 16 h/day for 4 consecutive days in each week) inhalation, and memory of the escape hole was evaluated. Following re-acquisition of the task, reversal learning was evaluated by moving the escape hole to the diametrically opposite location on the maze. Mice were exposed to an additional week of air or CIE inhalation and re-trained on the task, and then their ability to switch from a spatial to a visual-cued strategy was tested by changing the location of the escape hole at each trial and signaling its location with a proximal cue. **B:** Cognitive performance measured by path length, i.e., distance traveled from starting point to escape hole. Data were analyzed by repeated measures ANOVA within each experimental phase and at each phase transition and results are reported in the main text (Air, n=14 mice; CIE, n=11 mice). Data are presented as mean ± SEM. * represents the effect of trials, # represents the effect of treatment. One symbol, $p<0.05$; three symbols, $p<0.001$.

Supplementary Figure S1. To pharmacologically isolate the AMPA receptor-mediated component of sEPSCs, the NMDA receptor antagonist DL-AP5 (30 µM) was co-applied to cells bathed in GABA receptor antagonists (1 µM CGP 55845A and 30 µM bicuculline). DL-AP5 had no effect on sEPSC frequency, amplitude and kinetics (n=16 cells from both mPFC subregions of Air and CIE mice).

Supplementary Figure S2. Effect of CIE on spatial reference memory retention and cognitive flexibility in the Barnes maze. A: Cognitive performance measured by latency to enter escape hole. **B:** Cognitive performance measured by number of holes

visited prior to escape. Data were analyzed by repeated measures ANOVA within each experimental phase and at each phase transition and results are reported in Tables S1 and S2 (Air, n=14 mice; CIE, n=11 mice). Data are presented as mean ± SEM. * represents the effect of trials, # represents the effect of treatment. One symbol, $p<0.05$; two symbols, $p<0.01$; three symbols, $p<0.001$.

Table S1. Statistical analysis of latency to escape in the Barnes maze experiment. Data were analyzed by repeated measures ANOVA using trial as within-subject variable and treatment as between-subject variable. Data are shown in Supplementary Figure S2A.

Table S2. Statistical analysis of number of holes visited in the Barnes maze experiment. Data were analyzed by repeated measures ANOVA using trial as within-subject variable and treatment as between-subject variable. Data are shown in Supplementary Figure S2B.

Acknowledgements:

We thank Dr. Michal Bajo from the Department of Neuroscience at The Scripps Research Institute and Dr. Attila Szucs from the Department of Physiology and Neurobiology at Eötvös Lóránd University and the BioCircuits Institute at University of California San Diego for their assistance with electrophysiological data analysis. This work was supported by National Institute on Alcohol Abuse and Alcoholism (NIH/NIAAA) grants K99 AA025408 (FPV), T32 AA007456 (HS), F32 AA024952 (HS), U01 AA013498 (MR), R01 AA021491 (MR), R21 AA024198 (CC), and P60 AA006420 (MR and CC), as well as the Pearson Center for Alcoholism and Addiction Research.

Conflict of interest: none

References

American Psychiatric Association (2013). Diagnostic and statistical manual of mental disorders, 5th edn (Arlington, VA: American Psychiatric Publishing).

Bach ME, Hawkins RD, Osman M, Kandel ER, Mayford M (1995) Impairment of spatial but not contextual memory in CaMKII mutant mice with a selective loss of hippocampal LTP in the range of the theta frequency. *Cell* 81, 905-915.

Badanich KA, Becker HC, Woodward JJ (2011) Effects of chronic intermittent ethanol exposure on orbitofrontal and medial prefrontal cortex-dependent behaviors in mice. *Behav Neurosci* 125, 879-891.

Bajo M, Varodayan FP, Madamba SG, Robert AJ, Casal LM, Oleata CS, Siggins GR, Roberto M (2015) IL-1 interacts with ethanol effects on GABAergic transmission in the mouse central amygdala. *Front Pharmacol* 6, 49.

Balleine BW, Dickinson A (1998) Goal-directed instrumental action: contingency and incentive learning and their cortical substrates. *Neuropharmacology* 37, 407-419.

Barnes CA (1979) Memory deficits associated with senescence: a neurophysiological and behavioral study in the rat. *J Comp Physiol Psychol* 93, 74-104.

Becker HC, Lopez MF (2004) Increased ethanol drinking after repeated chronic ethanol exposure and withdrawal experience in C57BL/6 mice. *Alcohol Clin Exp Res* 28, 1829-1838.

Bitzenhofer SH, Ahlbeck J, Wolff A, Wiegert JS, Gee CE, Oertner TG, Hanganu-Opatz IL (2017) Layer-specific optogenetic activation of pyramidal neurons causes beta-gamma entrainment of neonatal networks. *Nat Commun* 8, 14563.

Bourne J, Harris KM (2007) Do thin spines learn to be mushroom spines that remember? *Curr Opin Neurobiol* 17, 381-386.

Brown VJ, Bowman EM (2002) Rodent models of prefrontal cortical function. *Trends Neurosci* 25, 340-343.

Burnett EJ, Chandler LJ, Trantham-Davidson H (2016) Glutamatergic plasticity and alcohol dependence-induced alterations in reward, affect and cognition. *Prog Neuropsychopharmacol Biol Psychiatry* 65, 309-320.

Cheriyan J, Kaushik MK, Ferreira AN, Sheets PL (2016) Specific Targeting of the Basolateral Amygdala to Projectionally Defined Pyramidal Neurons in Prelimbic and Infralimbic Cortex. *eNeuro* 3.

Chudasama Y, Robbins TW (2006) Functions of frontostriatal systems in cognition: comparative neuropsychopharmacological studies in rats, monkeys and humans. *Biol Psychol* 73, 19-38.

Coleman LG, Jr., He J, Lee J, Styner M, Crews FT (2011) Adolescent binge drinking alters adult brain neurotransmitter gene expression, behavior, brain regional volumes, and neurochemistry in mice. *Alcohol Clin Exp Res* 35, 671-688.

Coleman LG, Jr., Liu W, Oguz I, Styner M, Crews FT (2014) Adolescent binge ethanol treatment alters adult brain regional volumes, cortical extracellular matrix protein and behavioral flexibility. *Pharmacol Biochem Behav* 116, 142-151.

Contet C, Rawlins JN, Bannerman DM (2001) Faster is not surer--a comparison of C57BL/6J and 129S2/Sv mouse strains in the watermaze. *Behav Brain Res* 125, 261-267.

Cooney NL, Litt MD, Morse PA, Bauer LO, Gaupp L (1997) Alcohol cue reactivity, negative-mood reactivity, and relapse in treated alcoholic men. *J Abnorm Psychol* 106, 243-250.

Coutureau E, Killcross S (2003) Inactivation of the infralimbic prefrontal cortex reinstates goal-directed responding in overtrained rats. *Behav Brain Res* 146, 167-174.

Cyders MA, Dzemidzic M, Eiler WJ, Coskunpinar A, Karyadi K, Kareken DA (2014) Negative urgency and ventromedial prefrontal cortex responses to alcohol cues: FMRI evidence of emotion-based impulsivity. *Alcohol Clin Exp Res* 38, 409-417.

Dalley JW, Cardinal RN, Robbins TW (2004) Prefrontal executive and cognitive functions in rodents: neural and neurochemical substrates. *Neurosci Biobehav Rev* 28, 771-784.

Darcet F, Mendez-David I, Tritschler L, Gardier AM, Guilloux JP, David DJ (2014) Learning and memory impairments in a neuroendocrine mouse model of anxiety/depression. *Front Behav Neurosci* 8, 136.

de Bruin JP, Sanchez-Santed F, Heinsbroek RP, Donker A, Postmes P (1994) A behavioural analysis of rats with damage to the medial prefrontal cortex using the Morris water maze: evidence for behavioural flexibility, but not for impaired spatial navigation. *Brain Res* 652, 323-333.

de Castro V, Fong T, Rosenthal RJ, Tavares H (2007) A comparison of craving and emotional states between pathological gamblers and alcoholics. *Addict Behav* 32, 1555-1564.

De Koninck Y, Mody I (1994) Noise analysis of miniature IPSCs in adult rat brain slices: properties and modulation of synaptic GABAA receptor channels. *J Neurophysiol* 71, 1318-1335.

De Roo M, Klauser P, Garcia PM, Poglia L, Muller D (2008) Spine dynamics and synapse remodeling during LTP and memory processes. *Prog Brain Res* 169, 199-207.

Deacon RM, Bannerman DM, Kirby BP, Croucher A, Rawlins JN (2002) Effects of cytotoxic hippocampal lesions in mice on a cognitive test battery. *Behav Brain Res* 133, 57-68.

Deacon RM, Rawlins JN (2002) Learning impairments of hippocampal-lesioned mice in a paddling pool. *Behav Neurosci* 116, 472-478.

Delatour B, Gisquet-Verrier P (2000) Functional role of rat prelimbic-infralimbic cortices in spatial memory: evidence for their involvement in attention and behavioural flexibility. *Behav Brain Res* 109, 113-128.

DeNardo LA, Berns DS, DeLoach K, Luo L (2015) Connectivity of mouse somatosensory and prefrontal cortex examined with trans-synaptic tracing. *Nat Neurosci* 18, 1687-1697.

Dolan RJ, Dayan P (2013) Goals and habits in the brain. *Neuron* 80, 312-325.

Dupuy M, Chanraud S (2016) Imaging the Addicted Brain: Alcohol. *Int Rev Neurobiol* 129, 1-31.

Floresco SB, Block AE, Tse MT (2008) Inactivation of the medial prefrontal cortex of the rat impairs strategy set-shifting, but not reversal learning, using a novel, automated procedure. *Behav Brain Res* 190, 85-96.

Gabbott PL, Warner TA, Jays PR, Salway P, Busby SJ (2005) Prefrontal cortex in the rat: projections to subcortical autonomic, motor, and limbic centers. *J Comp Neurol* 492, 145-177.

Gass JT, Trantham-Davidson H, Kassab AS, Glen WB, Jr., Olive MF, Chandler LJ (2014) Enhancement of extinction learning attenuates ethanol-seeking behavior and alters plasticity in the prefrontal cortex. *J Neurosci* 34, 7562-7574.

George O, Koob GF (2010) Individual differences in prefrontal cortex function and the transition from drug use to drug dependence. *Neurosci Biobehav Rev* 35, 232-247.

Gourley SL, Taylor JR (2016) Going and stopping: dichotomies in behavioral control by the prefrontal cortex. *Nat Neurosci* 19, 656-664.

Harrison FE, Hosseini AH, McDonald MP (2009) Endogenous anxiety and stress responses in water maze and Barnes maze spatial memory tasks. *Behav Brain Res* 198, 247-251.

Heidbreder CA, Groenewegen HJ (2003) The medial prefrontal cortex in the rat: evidence for a dorso-ventral distinction based upon functional and anatomical characteristics. *Neurosci Biobehav Rev* 27, 555-579.

Holmes A, Fitzgerald PJ, MacPherson KP, DeBrouse L, Colacicco G, Flynn SM, Masneuf S, Pleil KE, Li C, Marcinkiewcz CA, Kash TL, Gunduz-Cinar O, Camp M (2012) Chronic alcohol remodels prefrontal neurons and disrupts NMDAR-mediated fear extinction encoding. *Nat Neurosci* 15, 1359-1361.

Holmes A, Wrenn CC, Harris AP, Thayer KE, Crawley JN (2002) Behavioral profiles of inbred strains on novel olfactory, spatial and emotional tests for reference memory in mice. *Genes Brain Behav* 1, 55-69.

Holscher C (1999) Stress impairs performance in spatial water maze learning tasks. *Behav Brain Res* 100, 225-235.

Hu W, Morris B, Carrasco A, Kroener S (2015) Effects of acamprosate on attentional set-shifting and cellular function in the prefrontal cortex of chronic alcohol-exposed mice. *Alcohol Clin Exp Res* 39, 953-961.

Irimia C, Buczynski MW, Natividad LA, Laredo SA, Avalos N, Parsons LH (2017) Dysregulated Glycine Signaling Contributes to Increased Impulsivity during Protracted Alcohol Abstinence. *J Neurosci* 37, 1853-1861.

Irimia C, Tuong RN, Quach T, Parsons LH (2014) Impaired response inhibition in the rat 5 choice continuous performance task during protracted abstinence from chronic alcohol consumption. *PLoS One* 9, e109948.

Irimia C, Wiskerke J, Natividad LA, Polis IY, de Vries TJ, Pattij T, Parsons LH (2015) Increased impulsivity in rats as a result of repeated cycles of alcohol intoxication and abstinence. *Addict Biol* 20, 263-274.

Jasinska AJ, Stein EA, Kaiser J, Naumer MJ, Yalachkov Y (2014) Factors modulating neural reactivity to drug cues in addiction: a survey of human neuroimaging studies. *Neurosci Biobehav Rev* 38, 1-16.

Johnson CN, Fromme K (1994) An experimental test of affect, subjective craving, and alcohol outcome expectancies as motivators of young adult drinking. *Addict Behav* 19, 631-641.

Jury NJ, DiBerto JF, Kash TL, Holmes A (2017a) Sex differences in the behavioral sequelae of chronic ethanol exposure. *Alcohol* 58, 53-60.

Jury NJ, Pollack GA, Ward MJ, Bezek JL, Ng AJ, Pinard CR, Bergstrom HC, Holmes A (2017b) Chronic Ethanol During Adolescence Impacts Corticolimbic Dendritic Spines and Behavior. *Alcohol Clin Exp Res* 41, 1298-1308.

Killcross S, Coutureau E (2003) Coordination of actions and habits in the medial prefrontal cortex of rats. *Cereb Cortex* 13, 400-408.

Kim A, Zamora-Martinez ER, Edwards S, Mandyam CD (2015) Structural reorganization of pyramidal neurons in the medial prefrontal cortex of alcohol dependent rats is associated with altered glial plasticity. *Brain Struct Funct* 220, 1705-1720.

Koob GF, Volkow ND (2016) Neurobiology of addiction: a neurocircuitry analysis. *Lancet Psychiatry* 3, 760-773.

Kroener S, Mulholland PJ, New NN, Gass JT, Becker HC, Chandler LJ (2012) Chronic alcohol exposure alters behavioral and synaptic plasticity of the rodent prefrontal cortex. *PLoS One* 7, e37541.

Lacroix L, White I, Feldon J (2002) Effect of excitotoxic lesions of rat medial prefrontal cortex on spatial memory. *Behav Brain Res* 133, 69-81.

Laguesse S, Morisot N, Shin JH, Liu F, Adrover MF, Sakhai SA, Lopez MF, Phamluong K, Griffin WC, 3rd, Becker HC, Bender KJ, Alvarez VA, Ron D (2017) Prosapip1-Dependent Synaptic Adaptations in the Nucleus Accumbens Drive Alcohol Intake, Seeking, and Reward. *Neuron* 96, 145-159 e148.

Latif-Hernandez A, Shah D, Ahmed T, Lo AC, Callaerts-Vegh Z, Van der Linden A, Balschun D, D'Hooge R (2016) Quinolinic acid injection in mouse medial

prefrontal cortex affects reversal learning abilities, cortical connectivity and hippocampal synaptic plasticity. *Sci Rep* 6, 36489.

Le Berre AP, Fama R, Sullivan EV (2017) Executive Functions, Memory, and Social Cognitive Deficits and Recovery in Chronic Alcoholism: A Critical Review to Inform Future Research. *Alcohol Clin Exp Res* 41, 1432-1443.

Lee E, Ku J, Jung YC, Lee H, An SK, Kim KR, Yoon KJ, Namkoong K (2013) Neural evidence for emotional involvement in pathological alcohol craving. *Alcohol Alcohol* 48, 288-294.

Little JP, Carter AG (2012) Subcellular synaptic connectivity of layer 2 pyramidal neurons in the medial prefrontal cortex. *J Neurosci* 32, 12808-12819.

Little JP, Carter AG (2013) Synaptic mechanisms underlying strong reciprocal connectivity between the medial prefrontal cortex and basolateral amygdala. *J Neurosci* 33, 15333-15342.

Livingston-Thomas JM, Jeffers MS, Nguemeni C, Shoichet MS, Morshead CM, Corbett D (2015) Assessing cognitive function following medial prefrontal stroke in the rat. *Behav Brain Res* 294, 102-110.

Maaswinkel H, Gispen WH, Spruijt BM (1996) Effects of an electrolytic lesion of the prelimbic area on anxiety-related and cognitive tasks in the rat. *Behav Brain Res* 79, 51-59.

McDonald RJ, King AL, Foong N, Rizos Z, Hong NS (2008) Neurotoxic lesions of the medial prefrontal cortex or medial striatum impair multiple-location place learning in the water task: evidence for neural structures with complementary roles in behavioural flexibility. *Exp Brain Res* 187, 419-427.

Metz AE, Yau HJ, Centeno MV, Apkarian AV, Martina M (2009) Morphological and functional reorganization of rat medial prefrontal cortex in neuropathic pain. *Proc Natl Acad Sci U S A* 106, 2423-2428.

Milad MR, Quirk GJ (2002) Neurons in medial prefrontal cortex signal memory for fear extinction. *Nature* 420, 70-74.

Miyakawa T, Yared E, Pak JH, Huang FL, Huang KP, Crawley JN (2001) Neurogranin null mutant mice display performance deficits on spatial learning tasks with anxiety related components. *Hippocampus* 11, 763-775.

Moorman DE, James MH, McGlinchey EM, Aston-Jones G (2015) Differential roles of medial prefrontal subregions in the regulation of drug seeking. *Brain Res* 1628, 130-146.

Morgan MA, LeDoux JE (1995) Differential contribution of dorsal and ventral medial prefrontal cortex to the acquisition and extinction of conditioned fear in rats. *Behav Neurosci* 109, 681-688.

Morris RG, Garrud P, Rawlins JN, O'Keefe J (1982) Place navigation impaired in rats with hippocampal lesions. *Nature* 297, 681-683.

Mulholland PJ, Chandler LJ (2007) The thorny side of addiction: adaptive plasticity and dendritic spines. *ScientificWorldJournal* 7, 9-21.

Myers-Schulz B, Koenigs M (2012) Functional anatomy of ventromedial prefrontal cortex: implications for mood and anxiety disorders. *Mol Psychiatry* 17, 132-141.

Navarro AI, Mandyam CD (2015) Protracted abstinence from chronic ethanol exposure alters the structure of neurons and expression of oligodendrocytes and myelin in the medial prefrontal cortex. *Neuroscience* 293, 35-44.

Oscar-Berman M, Marinkovic K (2007) Alcohol: effects on neurobehavioral functions and the brain. *Neuropsychol Rev* 17, 239-257.

Otis TS, De Koninck Y, Mody I (1994) Lasting potentiation of inhibition is associated with an increased number of gamma-aminobutyric acid type A receptors activated during miniature inhibitory postsynaptic currents. *Proc Natl Acad Sci U S A* 91, 7698-7702.

Oualian C, Gisquet-Verrier P (2010) The differential involvement of the prelimbic and infralimbic cortices in response conflict affects behavioral flexibility in rats trained in a new automated strategy-switching task. *Learn Mem* 17, 654-668.

Pava MJ, Woodward JJ (2014) Chronic ethanol alters network activity and endocannabinoid signaling in the prefrontal cortex. *Front Integr Neurosci* 8, 58.

Peters J, Kalivas PW, Quirk GJ (2009) Extinction circuits for fear and addiction overlap in prefrontal cortex. *Learn Mem* 16, 279-288.

Pfarr S, Meinhardt MW, Klee ML, Hansson AC, Vengeliene V, Schonig K, Bartsch D, Hope BT, Spanagel R, Sommer WH (2015) Losing Control: Excessive Alcohol Seeking after Selective Inactivation of Cue-Responsive Neurons in the Infralimbic Cortex. *J Neurosci* 35, 10750-10761.

Pleil KE, Lowery-Gionta EG, Crowley NA, Li C, Marcinkiewcz CA, Rose JH, McCall NM, Maldonado-Devincci AM, Morrow AL, Jones SR, Kash TL (2015) Effects of chronic ethanol exposure on neuronal function in the prefrontal cortex and extended amygdala. *Neuropharmacology* 99, 735-749.

Pombo S, Luisa Figueira M, Walter H, Lesch O (2016) Motivational factors and negative affectivity as predictors of alcohol craving. *Psychiatry Res* 243, 53-60.

Quirk GJ, Russo GK, Barron JL, Lebron K (2000) The role of ventromedial prefrontal cortex in the recovery of extinguished fear. *J Neurosci* 20, 6225-6231.

Ragozzino ME, Wilcox C, Raso M, Kesner RP (1999) Involvement of rodent prefrontal cortex subregions in strategy switching. *Behav Neurosci* 113, 32-41.

Sala C, Segal M (2014) Dendritic spines: the locus of structural and functional plasticity. *Physiol Rev* 94, 141-188.

Salling MC, Harrison NL (2014) Strychnine-sensitive glycine receptors on pyramidal neurons in layers II/III of the mouse prefrontal cortex are tonically activated. *J Neurophysiol* 112, 1169-1178.

Schweitzer P, Cates-Gatto C, Varodayan FP, Nadav T, Roberto M, Lasek AW, Roberts AJ (2016) Dependence-induced ethanol drinking and GABA neurotransmission are altered in Alk deficient mice. *Neuropharmacology* 107, 1-8.

Seamans JK, Lapish CC, Durstewitz D (2008) Comparing the prefrontal cortex of rats and primates: insights from electrophysiology. *Neurotox Res* 14, 249-262.

Seo D, Lacadie CM, Sinha R (2016) Neural Correlates and Connectivity Underlying Stress-Related Impulse Control Difficulties in Alcoholism. *Alcohol Clin Exp Res* 40, 1884-1894.

Shrestha P, Mousa A, Heintz N (2015) Layer 2/3 pyramidal cells in the medial prefrontal cortex moderate stress induced depressive behaviors. *Elife* 4.

Sinha R (2013) The clinical neurobiology of drug craving. *Curr Opin Neurobiol* 23, 649-654.

Smith CJ, Xiong G, Elkind JA, Putnam B, Cohen AS (2015) Brain Injury Impairs Working Memory and Prefrontal Circuit Function. *Front Neurol* 6, 240.

Sunyer B, Patil S, Höger H, Lubec G (2007) Barnes maze, a useful task to assess spatial reference memory in the mice.

Trantham-Davidson H, Burnett EJ, Gass JT, Lopez MF, Mulholland PJ, Centanni SW, Floresco SB, Chandler LJ (2014) Chronic alcohol disrupts dopamine receptor activity and the cognitive function of the medial prefrontal cortex. *J Neurosci* 34, 3706-3718.

Uylings HB, Groenewegen HJ, Kolb B (2003) Do rats have a prefrontal cortex? *Behav Brain Res* 146, 3-17.

Uys JD, McGuier NS, Gass JT, Griffin WC, 3rd, Ball LE, Mulholland PJ (2016) Chronic intermittent ethanol exposure and withdrawal leads to adaptations in nucleus accumbens core postsynaptic density proteome and dendritic spines. *Addict Biol* 21, 560-574.

Vertes RP (2004) Differential projections of the infralimbic and prelimbic cortex in the rat. *Synapse* 51, 32-58.

Vidal-Gonzalez I, Vidal-Gonzalez B, Rauch SL, Quirk GJ (2006) Microstimulation reveals opposing influences of prelimbic and infralimbic cortex on the expression of conditioned fear. *Learn Mem* 13, 728-733.

Wang GQ, Cen C, Li C, Cao S, Wang N, Zhou Z, Liu XM, Xu Y, Tian NX, Zhang Y, Wang J, Wang LP, Wang Y (2015) Deactivation of excitatory neurons in the prelimbic cortex via Cdk5 promotes pain sensation and anxiety. *Nat Commun* 6, 7660.

Whishaw IQ, Tomie J (1996) Of mice and mazes: similarities between mice and rats on dry land but not water mazes. *Physiol Behav* 60, 1191-1197.

Wills TA, Baucum AJ, 2nd, Holleran KM, Chen Y, Pasek JG, Delpire E, Tabb DL, Colbran RJ, Winder DG (2017) Chronic intermittent alcohol disrupts the GluN2B-associated proteome and specifically regulates group I mGlu receptor-dependent long-term depression. *Addict Biol* 22, 275-290.

Fig. 1

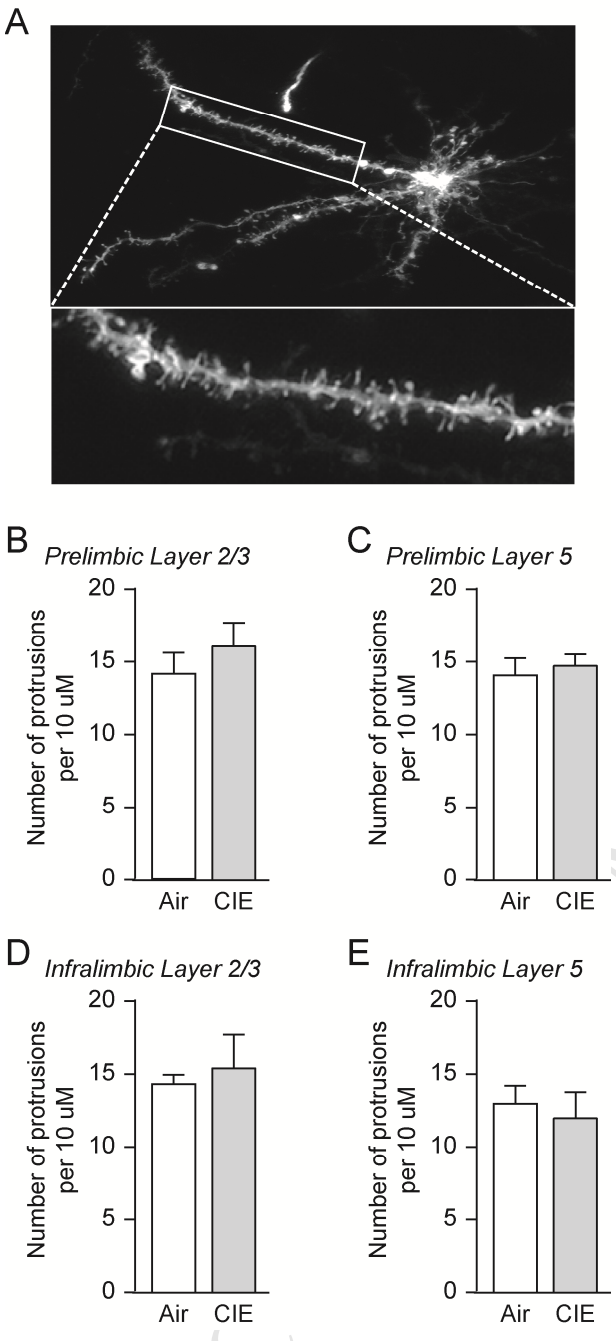

Fig. 2

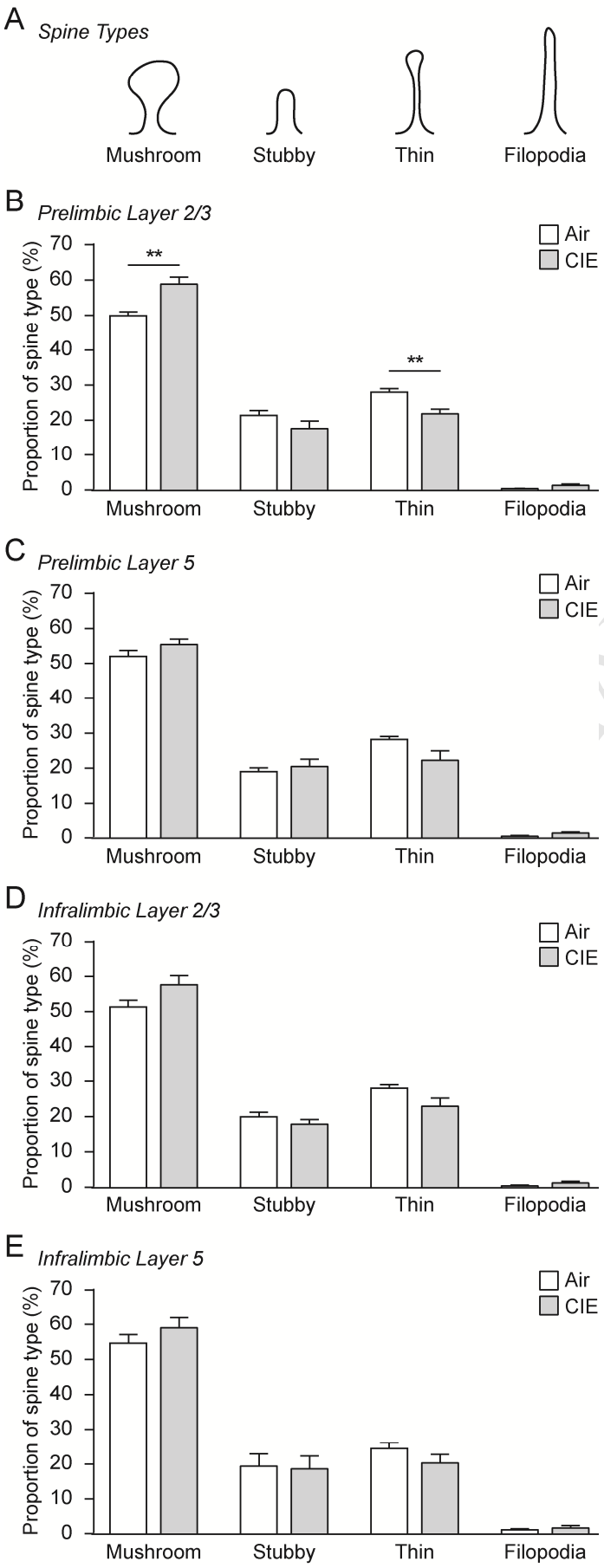
A
Spine Types
Mushroom
Stubby
Thin
Filopodia
B
Prelimbic Layer 2/3
Air
CIE
Proportion of spine type (%)
70
60
50
40
30
20
10
0
**
**
Mushroom
Stubby
Thin
Filopodia
C
Prelimbic Layer 5
Air
CIE
Proportion of spine type (%)
Mushroom
Stubby
Thin
Filopodia
D
Infralimbic Layer 2/3
Air
CIE
Proportion of spine type (%)
Mushroom
Stubby
Thin
Filopodia
E
Infralimbic Layer 5
Air
CIE
Proportion of spine type (%)
Mushroom
Stubby
Thin
Filopodia

Fig. 3

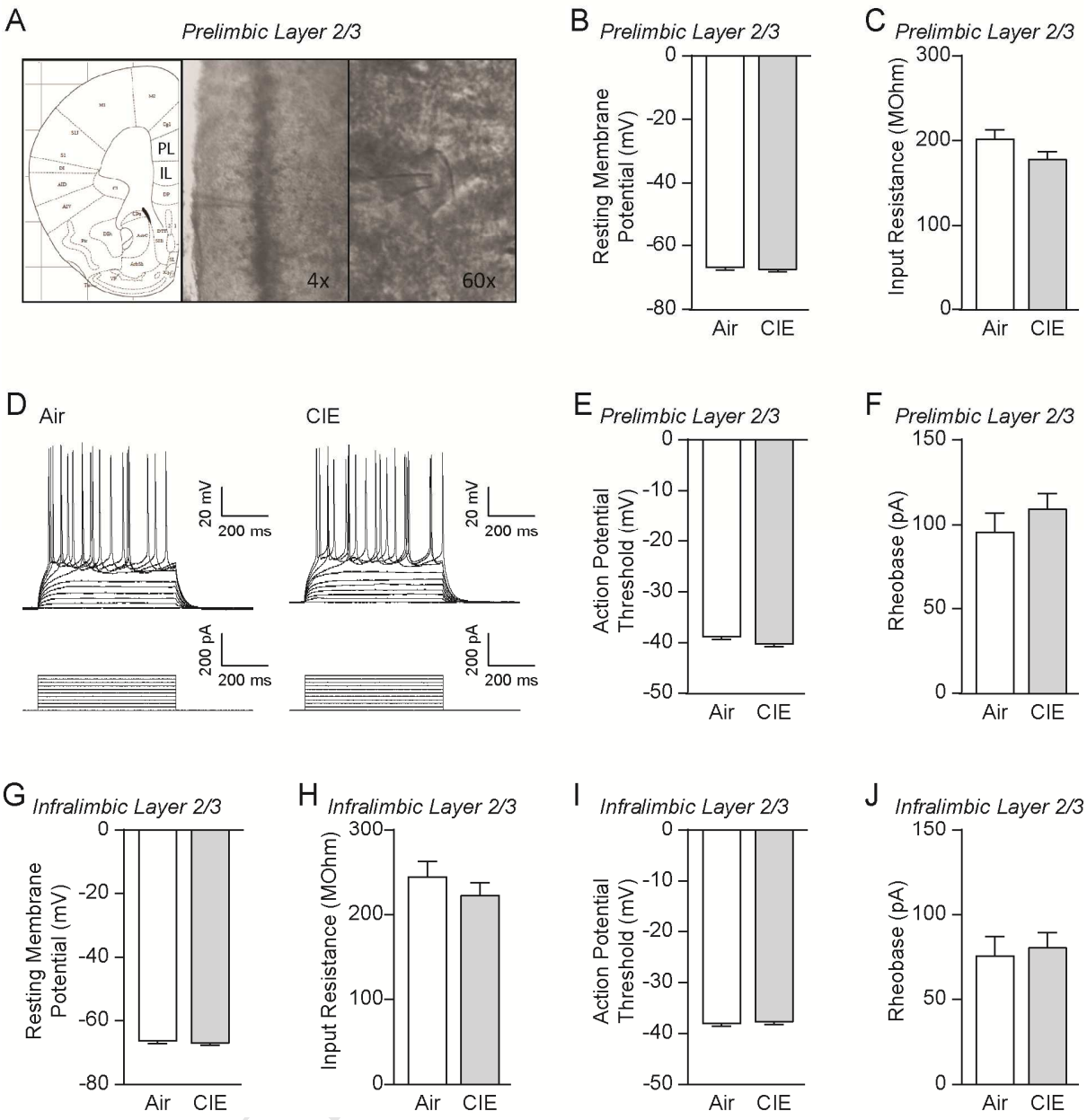
A
Prelimbic Layer 2/3
PL
IL
4x
60x
B
Prelimbic Layer 2/3
Resting Membrane Potential (mV)
0
-20
-40
-60
-80
Air
CIE
C
Prelimbic Layer 2/3
Input Resistance (MOhm)
300
200
100
0
Air
CIE
D
Air
CIE
20 mV
200 ms
200 pA
200 ms
E
Prelimbic Layer 2/3
Action Potential Threshold (mV)
0
-10
-20
-30
-40
-50
Air
CIE
F
Prelimbic Layer 2/3
Rheobase (pA)
150
100
50
0
Air
CIE
G
Infralimbic Layer 2/3
Resting Membrane Potential (mV)
0
-20
-40
-60
-80
Air
CIE
H
Infralimbic Layer 2/3
Input Resistance (MOhm)
300
200
100
0
Air
CIE
I
Infralimbic Layer 2/3
Action Potential Threshold (mV)
0
-10
-20
-30
-40
-50
Air
CIE
J
Infralimbic Layer 2/3
Rheobase (pA)
150
100
50
0
Air
CIE

Fig. 4

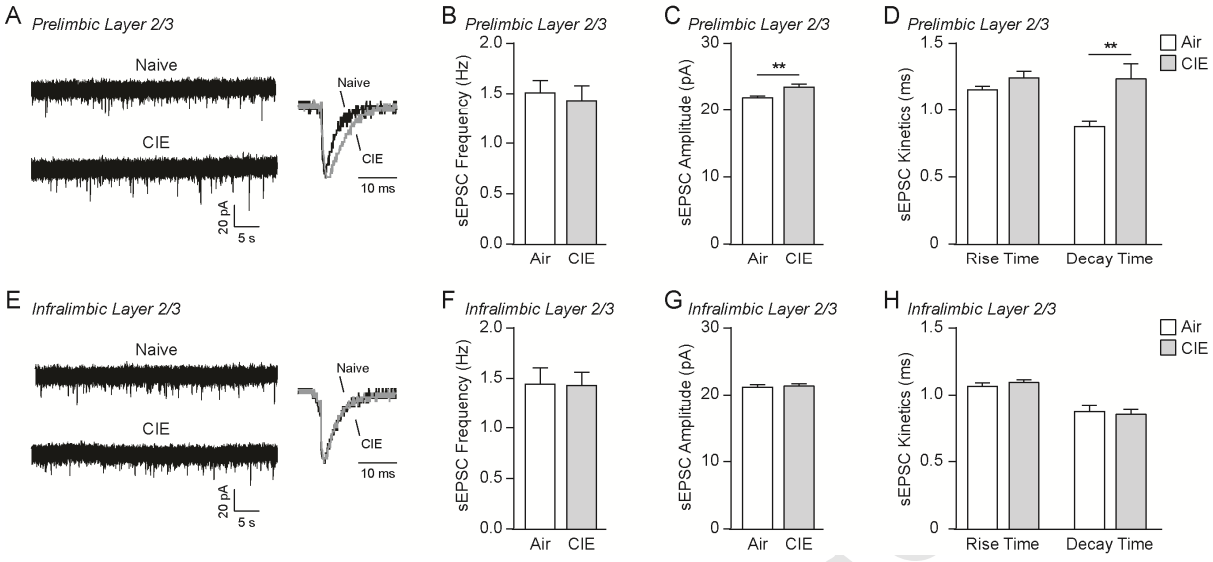

Fig. 5

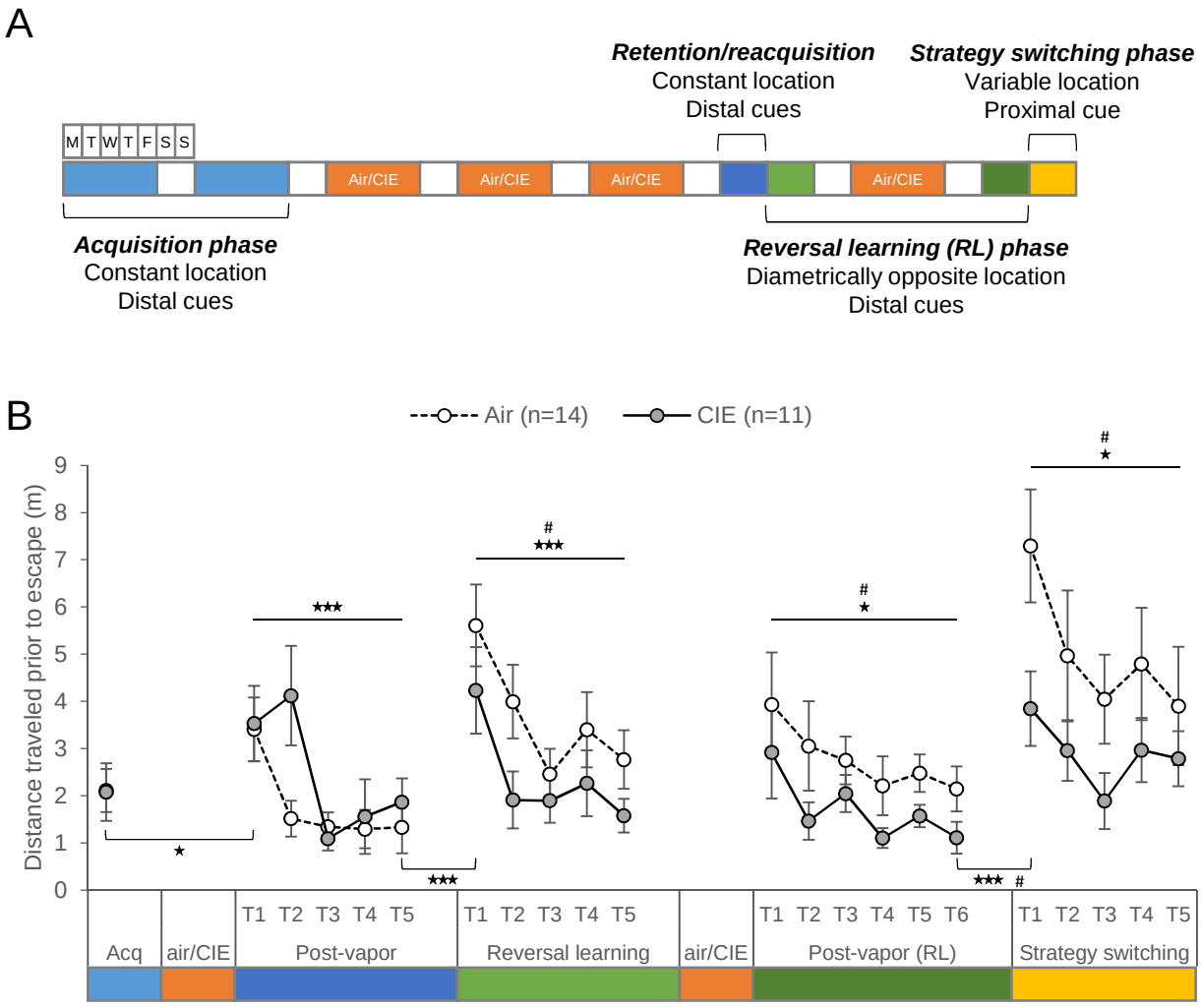
A
Retention/reacquisition
Constant location
Distal cues
Strategy switching phase
Variable location
Proximal cue
M T W T F S S
Air/CIE
Air/CIE
Air/CIE
Air/CIE
Acquisition phase
Constant location
Distal cues
Reversal learning (RL) phase
Diametrically opposite location
Distal cues
B
Air (n=14)
CIE (n=11)
Distance traveled prior to escape (m)
0
1
2
3
4
5
6
7
8
9
Acq
air/CIE
T1 T2 T3 T4 T5
Post-vapor
T1 T2 T3 T4 T5
Reversal learning
air/CIE
T1 T2 T3 T4 T5 T6
Post-vapor (RL)
T1 T2 T3 T4 T5
Strategy switching

Highlights

- Withdrawal from chronic intermittent ethanol alters the medial prefrontal cortex.
- It increases spine maturity in prelimbic cortex layer 2/3 pyramidal neurons.
- It also increases excitatory transmission in these neurons.
- However, it does not impair cognitive flexibility in the Barnes maze.